Coulomb Stress Analysis of the West Coast Sumatra Earthquake on Mount Imun and Mount Helatoba

Goldberd Harmuda Duva Sinaga*, Juliper Nainggolan, & Hebron Pardede
Physics Education Study Program, Universitas HKBP Nommensen, Indonesia
*Corresponding Author: goldberdhdsinaga@gmail.com

Received: 27th November 2024; **Accepted**: 11th March 2025; **Published**: 18th March 2025
DOI: https://dx.doi.org/10.29303/jpft.v11i1.8102

Abstract *- The island of Sumatra is a meeting area between the Indian Ocean plate in the South and the southwest edge of the Sunda Exposure, which is also the continental plate of Southeast Asia or the Eurasian Plate. The meeting of the plates makes the island of Sumatra an area prone to tectonic earthquakes, including Mount Imun and Helatoba which are located in the Tarutung basin. This study uses the Mohr-Coulomb model in the analysis of changes in coulomb stress. This modeling uses data from earthquakes that occurred on the West Coast of Sumatra which was then processed in coulomb 3.4 software. This modeling resulted in stress distribution in Imun and Helatoba. Coulomb stress changes until this time in Imun is 0.323 bar (2024) and coulomb stress change in Helatoba is 0.217 bar. The effect of the increase in coulomb stress (red lobe) originating from the earthquake on the west coast of Sumatra is triggering 2 tectonic earthquakes at the coordinates of Mount Imun in 2022 and triggering a tectonic earthquake at the coordinates of Helatoba in 2018.*

Keywords: *Coulomb Stress; Imun; Helatoba*

INTRODUCTION

The island of Sumatra is a meeting area between the Indian Ocean plate in the South and the southwest edge of the Sunda Exposure, which is also the continental plate of Southeast Asia or the Eurasian Plate. Until now, the allowance of the oceanic plate to the northeast is still active with an average speed of 6.3 cm/year of oceanic plate movement (Huchon & Pichon, 1984). The convergence of the Indian Plate and the Eurasian Plate is dominated by strike-slip tectonics. One of the consequences of the subsidy of the oceanic plate under the continental plate in the Sumatra area is the formation of the North Sumatra basin. The collision of the Indian Ocean plate in the south and the Eurasian continental plate in the north forms a tectonic environment and basins. The Sumatran Fault, which is parallel to the current subsidy zone and the tertiary subduction zone, is closely related to obligue subduction in Sumatran waters. (Deformasi et al., 2006)

The Tarutung Basin is located in North Central Sumatra, 30 km South of the giant Lake Toba caldera.The basin is15 km wide, 2.5 km long and extends in the NNW–SSE direction along the prominent NW–SE striking SFS, which represents a dextral strike–slip fault related to oblique subduction along the Sumatra arc (Sieh & Natawidjaja, 2000)(Muraoka et al., 2010). From the plate tectonic perspective, theTarutung Basin is located at the cross point of the SFS (Sumatera Fault System) and the Medial Sumatra Tectonic Zone (MSTZ) which separates the East from the West Sumatra block from Late Permianto early Triassic (Huchon & Pichon, 1984)

The Tarutung Basin is not typically rhombroedric shaped as one could expect for a pull-apart basin. Instead, it is more eye shaped possibly caused by anastomizing segments of the SFS. Two older volcanic centres are located at both ends of the Tarutung Basin. Mount Imun located at the northern end of the Tarutung Basin as an inactivevolcano with similar eruptiva (vesicular dacite) as the prominent Toba

Tuff (Aldiss & Ghazali, 1984) The morphology of Mount Imun is not cross cut by faults of the SFS indicating a young age presumable similaras Martimbang to the south of the basin. (Gasparon, 2005)

The geological conditions and movement of these plates have resulted in the island of Sumatra, especially Tarutung and its surroundings (Mount Imun and Mount Helatoba) becoming an area that often experiences tectonic earthquakes. Although earthquakes cannot be detected or predicted, earthquakes can be predicted by coulomb stress modeling. Coulomb stress modeling has been widely used to see the distribution area of earthquakes due to the main earthquake that occurred. Modelling has been widely used both in flat areas and in volcanoes. Coulomb stress modeling has been used in North Sumatra, especially Mount Sibayak (Sinaga et al., 2022), Sinabung (Kototabang & Geofisika, 2013)(Goldberd Harmuda Duva Sinaga et al., 2022), Toba (Sinaga & Nainggolan, 2023), Sibualbuali and Lubukraya (Sinaga et al., 2024), Sorikmarapi (Sinaga et al., 2021) and other areas such as Rinjani (Utama et al., 2020), Nias (Hughes et al., 2010), Aceh, Soputan and Gamalama (Sinaga et al., 2017), Maluku (Siwi et al., 2020), Java (Mala et al., 2020). Currently, Mount Imun and Helatoba are not included in the PVMBG monitoring. However, it does not mean that in the future, it is not impossible that these two mountains will receive special attention regarding volcanic activity. Although these two mountains have not shown volcanic activity, the geological stress conditions in these two mountains need to be analyzed. This is because these two mountains are located in the stress distribution area of Mount Toba with Mount Lubukraya and Sibualbuali. So in this case, the study will use coulomb stress modeling to look at the impact of earthquakes on the west coast of Sumatra on Immunity and Helatoba.

RESEARCH METHODS

This study uses the method used in the research on Mount Imun and Helatoba is an analytical-descriptive method. The model used in this study is the Coulomb Stress Model. Earthquake stress/strain will be analyzed in coulomb 3.4 software. The values and stress/strain distribution of the earthquake will be mapped in 2D and 3D using Global Mapping Tool Software and Google Earth Software. The data used in this study are data on earthquake magnitude and coordinates, earthquake depth, earthquake type (strike, slip, dip), and tensor moment. (Toda, 2005)

Considering the collapse of the fracture as a combined cause between normal (reduced) and shear stress conditions, it is measured as a static stress coulomb stress stress criterion (King et al., 1994). Changes in static coulomb stress caused by earthquakes can help explain the distribution of aftershocks (Parsons et al., 1999), as aftershocks will occur when coulomb stress exceeds the collapse force of the fault surface. The change in voltage of the Coulomb state (ΔCFF) is defined as

$$\Delta CFF = \Delta\tau + \mu\,(\Delta\sigma + \Delta p) \qquad (1)$$

Δ_τ represents the change in shear stress on the fault (positive in the slip direction), Δ_σ is the change in normal stress (positive for unsqueezed faults), Δp is the change in pressure pore, and μ is the coefficient of friction, which ranges from 0.6 to 0.8 for most intact rocks (Harris, 1998). In Oklahoma, where fluid injection is 1-2 km deep near the epicenter, and this has been used for disposal since 1993 (Keranen et al., 2013). In addition, the effect of pore pressure cannot be ignored either. The change in pore pressure after the change in tension occurs and there is no fluid flow (undrained condition), is

$$\Delta p = \frac{\beta \Delta \sigma_{kk}}{3} \quad (2)$$

where β is Skempton's coefficient and σkk is the sum of the diagonal elements of the stress tensor (Rice, 1992). Skempton's coefficient describes the change in pore pressure resulting from an externally applied voltage change, and often ranges in value from 0.5 to 1.0 (Green & Wang, 1986)(Hart & Wang, 1995)(Cocco, 2002). For fault zone rheology, where the fault of the zone material is tougher than the surrounding material, $\sigma_{xx}=\sigma_{yy}=\sigma_{zz}$ (Rice, 1992) (Parsons et al., 1999)(Harris, 1998); so, $\frac{\Delta\sigma_{kk}}{3} = \Delta_{\sigma}$. Equations (1) and (2) combined with this assumption, making

$$\Delta CFF = \Delta\tau + \mu\,\Delta\sigma \quad (3)$$

where $\mu' = \mu(1-\beta)$, the effective coefficient of friction. The effective coefficient of friction generally ranges from 0.0 to 0.8, but it is usually found around 0,4 (μ = 0,75, β = 0,47) for horizontal faults or faults of unknown orientation (Parsons et al., 1999). These values are commonly used in the calculation of coulomb voltage changes to minimize uncertainty. The location and geometry of the fault source, as well as the division of the slip over the plane source, play an important role in calculating the change in coulomb stress. Based on the magnitude of the earthquake, we model the source geometry with empirical relationships for strike-slip errors (Wells, Donald L.Coppersmith, 1994), which is built into Coulomb Software 3.3 (Toda, 2005).

RESULTS AND DISCUSSION

Results

This study uses ΔCFS modeling which was carried out to determine the distribution of static stress by earthquake events on Mount Imun and Helatoba. The Mohr-Coulomb model is also used to look at the relationship between earthquakes that can trigger the next earthquake, both between mainshock-mainshock and mainshock-aftershock, and the relationship between tectonic and volcanic earthquakes. (Utama et al., 2020). The Mohr-Coulomb model is simulated in coulomb 3.4 software which requires earthquake data in the form of magnitude moment, depth, longitude, and latitude obtained from the website of the Meteorology and Geophysics Agency (BMKG) while the focal mechanism is downloaded from the United States Geological Survey (USGS). The input data analyzed is earthquakes that occurred from August 2004 to August 2024 with no minimum magnitude moment. The study only selected earthquake data of at least 5.5 Mw with a radius of 200 km from Imun and Helatoba. This selection was made because Coulomb 3.4 has limited data input. This study uses the 2004-2024 earthquake data range so that the results of the coulomb stress change analysis are more accurate.

Table 1. ΔCFS in Mount Imun Depth 0-10 km in August 2004-August 2008

	2004	2005	2006	2007	2008
shear	0	-0,385	-0,385	-0,771	-0,771
normal	0	0,126	0,126	0,126	0,124
coulomb	0	0,122	0,122	0,122	0,121

Table 2. ΔCFS in Mount Imun August 2009-August 2013

	2009	2010	2011	2012	2013
shear	-0,771	-0,857	-0,861	-0,861	-0,861
normal	0,124	0,577	0,587	0,587	0,588
coulomb	0,121	0,216	0,216	0,216	0,216

Table 3. ΔCFS in Mount Imun August 2014-August 2018

	2014	2015	2016	2017	2018
shear	-0,861	-0,861	-0,861	-0,861	-0,860
normal	0,589	0,589	0,589	0,589	0,593
coulomb	0,216	0,216	0,216	0,216	0,218

Table 4. ΔCFS in Mount Imun August 2019-August 2024

	2019	2020	2021	2022	2023	2024
shear	-0,861	-0,861	-0,861	-0,840	-0,842	-0,842
normal	0,594	0,594	0,594	0,806	0,808	0,808
coulomb	0,218	0,218	0,218	0,324	0,323	0,323

Table 5. ΔCFS at Mount Helatoba, August 2004-August 2008

	2004	2005	2006	2007	2008
shear	0	-0,431	-0,431	-0,432	-0,432
normal	0	0,138	0,138	0,141	0,141
coulomb	0	0,121	0,121	0,121	0,121

Table 6. ΔCFS at Mount Helatoba, August 2009-August 2013

	2009	2010	2011	2012	2013
shear	-0,432	-0,329	-0,328	-0,328	-0,328
normal	0,141	0,165	0,185	0,185	0,186
coulomb	0,121	0,234	0,243	0,243	0,243

Table 7. ΔCFS at Mount Helatoba, August 2014-August 2018

	2014	2015	2016	2017	2018
shear	-0,328	-0,328	-0,328	-0,328	-0,327
normal	0,187	0,187	0,187	0,187	0,191
coulomb	0,243	0,243	0,243	0,243	0,246

Table 8. ΔCFS at Mount Helatoba, August 2019-August 2024

	2019	2020	2021	2022	2023	2024
shear	-0,327	-0,327	-0,327	-0,336	-0,338	-0,338
normal	0,194	0,194	0,194	0,150	0,151	0,151
coulomb	0,247	0,247	0,247	0,219	0,217	0,217

Discussion

Mount Imun

Table 1 shows the average values of normal, shear, and changes in coulomb stress that occur on Mount Imun at a depth of 0-10 km. The selection of this depth is because the average depth of Mount Merapi's magma is 10 km. The highest average normal value occurred in 2005 at 0.1269 bar while the lowest average normal value occurred in 2008 at -0.124 bar. The highest average shear value occurred in 2005 at -0.385 bar while the lowest average shear value occurred in 2007 at -0.771 bar. The average value of the largest change in coulomb stress occurred in 2005 at 0.122 bar while the average value of the smallest change in coulomb stress occurred in 2008 at 0.121 bar.

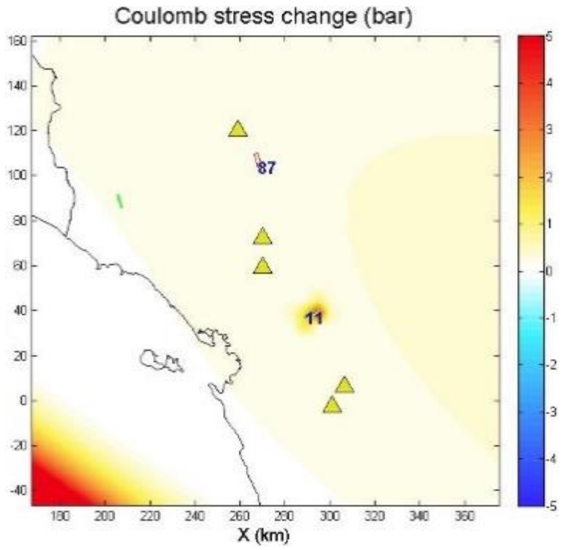

Figure 1. Changes in Mount Imun and Helatoba Stress Coulomb in 2005 (without involving the Aceh earthquake)

The magnitude of the average value of the change in coulomb stress that occurred in 2005 was caused by a large earthquake that occurred on December 26, 2004 in the Indian Ocean with a magnitude moment criterion of 9.1 Mw with a depth of 10 km km and was located at a longitude of 98.58^o, Latitude 3,316^o and type focal mechanism reverse fault.(Nursalam, 2016 & Fallis, 2013)

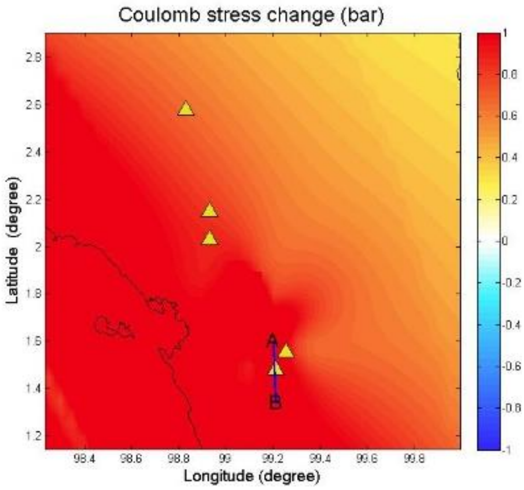

Figure 2. Changes in Mount Imun and Helatoba Stress Coulomb in 2005 (involving the Aceh earthquake)

The emergence of these major earthquakes resulted in many aftershocks that occurred in 2005. Figure 1 shows the change in coulomb stress that occurred in 2005 in Mount Imun and Helatoba. Changes in coulomb stress in 2005 only used 95 earthquake data with latitude limits of -3.5°-6.5° and longitude 91.5°-101.5° (not involving the Aceh earthquake) so that if this study is compared to other studies (Sinaga et al., 2024), there is a big difference in the scope of the spread of coulomb stress that is smaller than the change in coulomb stress involving the Aceh earthquake on December 26, 2024 in the analysis in software 3.4 (figure 2). The number of earthquakes analyzed greatly affects the red and blue lobes, but the change in coulomb stress affects the distribution of subsequent earthquakes to Mount Imun and Helatoba.

Table 2 shows the analysis of changes in coulomb stress from 2004-2013 that occurred on Mount Imun at a depth of 0-10 km. The highest average normal value occurred in 2011 at 0.587 bar while the lowest average normal value occurred in 2009 at 0.124 bar. The highest average shear value occurred in 2009 at -0.771 bar while the lowest average shear value occurred in 2013 at -0.861 bar.

The average value of the largest change in coulomb stress occurred in 2011 at 0.216 bar, while the average value of the smallest change in coulomb stress occurred in 2009 at 0.121 bar. Decrease in coulomb stress caused by 1 earthquake event closest to Imun in the north of Lake Toba waters (2009).

Table 3 shows the average values of normal, shear, and changes in coulomb stress that occur on Mount Imun at a depth of 0-10 km. The highest average normal value occurred in 2018 at 0.593 bar while the lowest average normal value occurred in 2014 at 0.589 bar. The highest average shear value occurred in 2018 at -0.860 bar while the lowest average shear value occurred in 2014 at -0.861 bar.

The average value of the largest change in coulomb stress occurred in 2018 at 0.218 bar while the average value of the smallest change in coulomb stress occurred in 2015 at 0.216 bar. The decrease in coulomb stress in the area was caused by 2 earthquakes in the north of Lake Toba waters in 2014 and 2017.

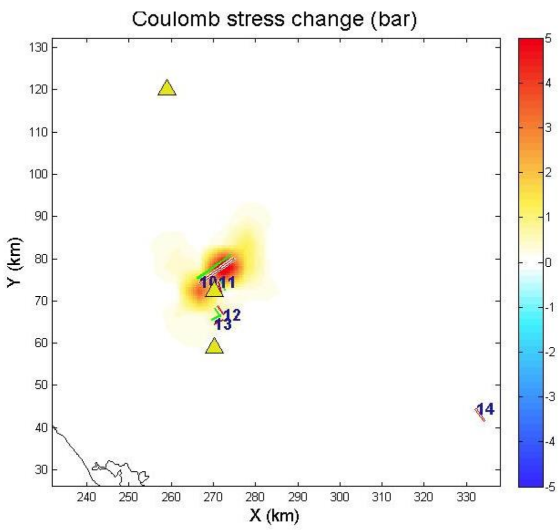

Figure 3. Earthquake coordinates on Mount Imun and changes in coulomb stress in 2022

Table 4 shows the average values of normal, shear, and changes in coulomb stress in Mount Imun at a depth of 0-10 km.

The highest normal average value occurred in 2022 of 0.806 bar while the lowest normal average value occurred in 2019 of 0.594 bar. The highest average shear value occurred in 2022 at -0.840 bar while the lowest average shear value occurred in 2019 at -0.861 bar. The average value of the largest change in coulomb stress occurred in 2022 at 0.324 bar while the average value of the smallest change in coulomb stress occurred in 2019 at 0.218 bar.

There is an interesting phenomenon that occurred in 2022 where tectonic earthquakes occurred right on Mount Imun 2 times. The first earthquake occurred on September 30, 2022 with a magnitude of 5.8 Mw at a depth of 16 km (focal mechanism strike-slip) and the second earthquake occurred on the same day but with a magnitude of 4.9 Mw at a depth of 12 km (focal mechanism strike-slip). The regional stress field is characterized by N–S oriented maximum horizontal stress and E–W oriented minimum horizontal stress in a strike–slip stress regime with the vertical stress being the intermediate principal stress (Cattin et al., 2009). The fault pattern of the Tarutung Basin is dominated by NW–SE striking faults parallel to the SFS, subordinately by E–W and N–S striking faults. Although both earthquakes occurred in a shallow depth range, they did not necessarily increase the change in coulomb stress. This is due to the angle of the focal mechanism that makes the Immune region experience strains until 2024.

Mount Helatoba

Table 5 shows the average values of normal, shear, and changes in coulomb stress on Mount Imun at a depth of 0-10 km. The normal average value occurred from 2005 to 2008 at 0.138 bar. This is because from 2005 to 2008, the normal average value did not change. The highest average shear value occurred in 2005 at -0.431 bar while the lowest average shear value occurred in 2007 at -0.432 bar.

The average value of the largest change in coulomb stress occurred in 2005 at 0.121 bar while the average value of the smallest change in coulomb stress occurred in 2008 at 0.121 bar. Mount Helatoba has a fairly close distance from Imun so that these two volcanic mountains have the same characteristics of increasing coulomb stress, which was caused by the Aceh earthquake of December 26, 2024.(Nursalam, 2016 & Fallis, 2013).

Table 6 shows the average values of normal, shear, and changes in coulomb stress in Mount Imun at a depth of 0-10 km. The highest normal average value occurred in 2010 at 0.165 bar while the lowest normal average value occurred in 2009 at 0.141 bar. The highest average shear value occurred in 2011 at -0.328 bar while the lowest average shear value occurred in 2009 at -0.432 bar.

The average value of the largest change in coulomb stress occurred in 2011 at 0.243 bar while the average value of the smallest change in coulomb stress occurred in 2009 at 0.121 bar. The decline in shear, normal, and coulomb was due to a decrease in the number of earthquakes that occurred. The nearest earthquakes only occurred 4 times in the southeast of Helatoba in 2010, 2011, 2012, and 2013.

Table 7 shows the average values of normal, shear, and changes in coulomb stress on Mount Imun at a depth of 0-10 km. The highest normal average value occurred in 2018 at 0.191 bar while the lowest normal average value occurred in 2014 at 0.187 bar. The highest average shear value also occurred in 2018 at -0.327 bar while the lowest average shear value also occurred in 2014 at -0.328 bar.

The average value of the largest change in coulomb stress still occurred in

2018 at 0.246 bar while the average value of the smallest change in coulomb stress occurred in 2014 at 0.243 bar. Earthquakes that occurred until 2014 provided a positive distribution of stress coulomb on Mount Helatoba. The red lobe gives a sign that the area has the potential for aftershocks. The distribution is evidenced by the occurrence of a tectonic earthquake just below Mount Helatoba at a depth of 130.7 km with a magnitude of 5.2 Mw. (focal mechanism strike-slip).

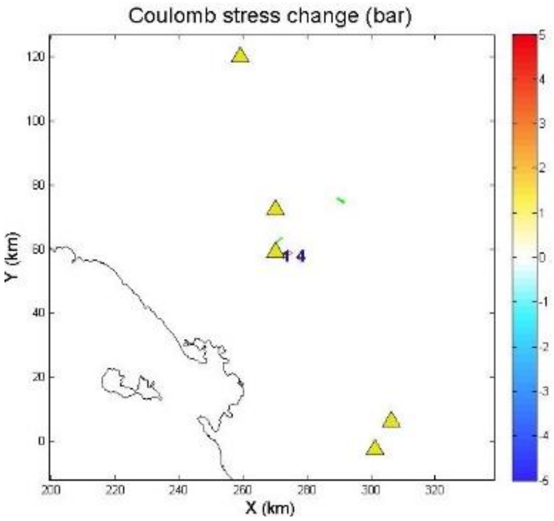

Figure 3. Coordinates of tectonic earthquakes in Helatoba

Figure 3 shows that the distribution of coulomb stress in 2017 has a significant impact (red lobe) on Helatoba. The influence was 2 events, namely the first tectonic earthquake right in Helatoba with a magnitude of 5.0 Mw and a depth of 19.4 km (focal mechanism strike-slip) on February 24, 2018 and the second tectonic earthquake also right in Helatoba with a magnitude of 4.9 Mw and a depth of 126.1 km (focal mechanism strike-slip) on March 13, 2018. As a result, Helatoba has the highest coulomb stress change value in 2018 since 2014. (table 7)

Table 8 shows the average values of normal, shear, and changes in coulomb stress on Mount Imun at a depth of 0-10 km. The highest normal average value occurred in 2019 at 0.194 bar while the lowest normal average value occurred in 2024 at 0.150 bar. The highest average shear value occurred in 2023 at -0.338 bar while the lowest average shear value occurred in 2019 at -0.327 bar.

The average value of the largest change in coulomb stress occurred in 2019 at 0.247 bar, while the average value of the smallest change in coulomb stress occurred in 2022 at 0.219 bar. The small change in coulomb stress from 2019-2024 was triggered by the lack of earthquake events that occurred in this time range.

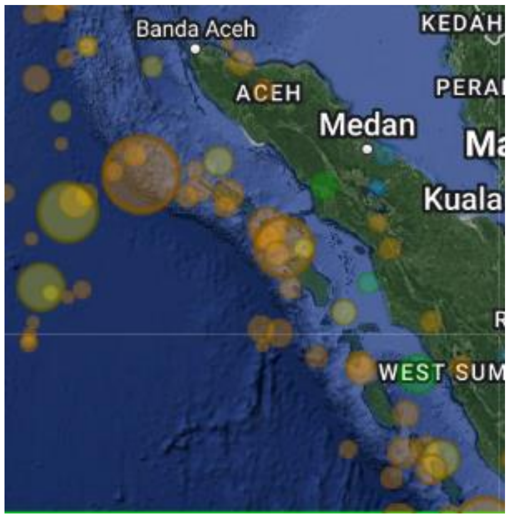

Figure 4. earthquakes that occurred on the west coast from August 2004 to August 2024

The earthquakes that occurred were only 9 incidents with a distance of >50 km. (waters of Lake Toba and Sorikmarapi). In addition, earthquakes that occur at the Imun coordinates also do not affect because of the angle of the focal mechanism strike slip that provides strain. The number of earthquakes that occurred from August 2004 to August 2024 was 1024 events. (table 4)

CONCLUSION

Earthquakes that occurred on the west coast of Sumatra resulted in changes in coulomb stress characterized by red lobes on Mount Imun and Helatoba. The effect of changes in coulomb stress on Imun and

Helatoba is that Mount Imun experienced a tectonic earthquake in 2022 and Helatoba also experienced tectonic earthquakes in 2015 and 2018. Although the impact of the west coast earthquake of Sumatra did not have a major impact, this area must still receive attention because this volcano is located between two residential areas. For further research, it is expected to analyze dynamic stress to calculate the stress value on the volcano.

ACKNOWLEDGMENT

The researcher expressed his gratitude to BMKG, USGS, Global CMT, GMT, and Google Earth for providing earthquake data and mapping.

REFERENCES

Aldiss, D. T., & Ghazali, S. A. (1984). The regional geology and evolution of the Toba volcano-tectonic depression, Indonesia. *Journal of the Geological Society*, *141*(3), 487–500. https://doi.org/10.1144/gsjgs.141.3.0487

Cattin, R., Pubellier, M., Rabaute, A., Delescluse, M., Vigny, C., Fleitout, L., & Dubernet, P. (2009). *Stress change and effective friction coefficient along the Sumatra-Andaman-Sagaing fault system after the 26 December 2004 (M*. https://doi.org/10.1029/2008GC002167

Cocco, M. (2002). Pore pressure and poroelasticity effects in Coulomb stress analysis of earthquake interactions. *Journal of Geophysical Research*, *107*(B2). https://doi.org/10.1029/2000jb000138

Deformasi, P., Mendatar, P., Pembentukan, T., Kecil, C., Di, P., Barat, S., & Jambi, D. A. N. (2006). *Peran deformasi pensesaran mendatar terhadap pembentukan beberapa cekungan kecil paleogen di sumatera barat dan jambi*. *XVI*(4), 232–240.

Gasparon, M. (2005). Quaternary volcanicity. *Geological Society Memoir*, *31*, 120–130. https://doi.org/10.1144/GSL.MEM.2005.031.01.09

Goldberd Harmuda Duva Sinaga, Switamy Angnitha Purba, & Ady Frenly Simanullang. (2022). Coulomb Stress Analysis And Monte Carlo Simulation In Predicting Sinabung Pyroclastic Flow. *World Journal of Advanced Research and Reviews*, *13*(1), 781–792. https://doi.org/10.30574/wjarr.2022.13.1.0085

Green, D. H., & Wang, H. F. (1986). *ap*. *51*(4), 948–956.

Harris, R. A. (1998). Introduction to special section: Stress triggers, stress shadows, and implications for seismic hazard. *Journal of Geophysical Research: Solid Earth*, *103*(10), 24347–24358. https://doi.org/10.1029/98jb01576

Hart, D. J., & Wang, H. F. (1995). limestone of the pore E = all K •,. *Journal of Geophysical Research : Solid Earth*, *100*(95), 741–751.

Huchon, P., & Pichon, X. Le. (1984). *Sunda Strait and Central Sumatra fault*. *November*, 668–672.

Hughes, K. L. H., Masterlark, T., & Mooney, W. D. (2010). Poroelastic stress-triggering of the 2005 M8.7 Nias earthquake by the 2004 M9.2 Sumatra-Andaman earthquake. *Earth and Planetary Science Letters*, *293*(3–4), 289–299. https://doi.org/10.1016/j.epsl.2010.02.043

Keranen, K. M., Savage, H. M., Abers, G. A., & Cochran, E. S. (2013). Potentially induced earthquakes in Oklahoma, USA: Links between wastewater injection and the 2011 Mw 5.7 earthquake sequence. *Geology*, *41*(6), 699–702.

https://doi.org/10.1130/G34045.1

King, G. C. P., Stein, R. S., & Jian Lin. (1994). Static stress changes and the triggering of earthquakes. *Bulletin - Seismological Society of America*, *84*(3), 935–953. https://doi.org/10.1016/0148-9062(95)94484-2

Kototabang, S. P. A. G. (GAW) B., & Geofisika, B. M. K. dan. (2013). Hubungan Antara Gempabumi Dengan Erupsi Gunungapi Studi Kasus Erupsi Gunung Sinabung Tahun 2010 Dan 2013. *Megasains*, *4*(Desember 2013), 117 – 123.

Mala, H. U., Mohamad, J. N., & Putra, V. G. V. (2020). *Identifikasi Pola Distribusi Stress Coloumb Pada Gempabumi 2 Agustus 2019 Di Tugu Hilir , Indonesia*. *5*(1).

Muraoka, H., Takahashi, M., Sundhoro, H., Dwipa, S., Soeda, Y., & Momita, M. (2010). *Geothermal Systems Constrained by the Sumatran Fault and Its Pull-Apart Basins in Sumatra , Western Indonesia*. *April*, 25–29.

Nursalam, 2016, metode penelitian, & Fallis, A. . (2013). 済無No Title No Title. *Journal of Chemical Information and Modeling*, *53*(9), 1689–1699.

Parsons, T., Stein, R. S., Simpson, R. W., & Reasenberg, P. A. (1999). Stress sensitivity of fault seismicity: A comparison between limited-offset oblique and major strike-slip faults. *Journal of Geophysical Research: Solid Earth*, *104*(B9), 20183–20202. https://doi.org/10.1029/1999jb900056

Rice, J. R. (1992). Fault Stress States, Pore Pressure Distributions, and the Weakness of the San Andreas Fault. *International Geophysics*, *51*(C), 475–503. https://doi.org/10.1016/S0074-6142(08)62835-1

Sieh, K., & Natawidjaja, D. (2000). Neotectonics of the Sumatran fault, Indonesia. *Journal of Geophysical Research: Solid Earth*, *105*(B12), 28295–28326. https://doi.org/10.1029/2000jb900120

Sinaga, G. H. D., Halawa, A., Prasetyo, R. A., & Alexander, I. J. (2024). *Coulomb Stress Changes in the 2004 Aceh Earthquake on the Mount Sibualbuali and Mount Lubukraya*. *10*(2).

Sinaga, G. H. D., Loeqman, A., Siagian, R. C., & Sinaga, M. P. (2022). Analysis of Coulomb Stress Changes in Aceh Earthquake on Sibayak Volcano. *Jurnal Pendidikan Fisika Dan Teknologi*, *8*(2), 217–227. https://doi.org/10.29303/jpft.v8i2.4409

Sinaga, G. H. D., & Nainggolan, J. (2023). Analysis of Sumatran Earthquake Coulomb Stress Changes in Geothermal Potential in Rianite, Samosir Regency. *Jurnal Pendidikan Fisika Dan Teknologi*, *9*(2), 224–233. https://doi.org/10.29303/jpft.v9i2.5900

Sinaga, G. H. D., Tambunan, M. R., Loeqman, A., & Wibowo, A. (2021). Coulomb Stress Change of the 2004 Aceh Earthquake on Mount Sorik Marapi 2021. *Jurnal Penelitian Fisika Dan Aplikasinya (JPFA)*, *11*(2), 158–170. https://doi.org/10.26740/jpfa.v11n2.p158-170

Sinaga, G. H. D., Zarlis, M., Sitepu, M., Prasetyo, R. A., & Simanullang, A. (2017). Coulomb stress analysis of West Halmahera earthquake mw=7.2 to mount Soputan and Gamalama volcanic activities. *IOP Conference Series: Earth and Environmental Science*, *56*(1), 3–10. https://doi.org/10.1088/1755-1315/56/1/012005

Siwi, P. W., Sriyanto, S. P. D., Rondonuwu, A. T., & Silangen, P. M. (2020). Perubahan Coulomb Stress Akibat Gempabumi Laut Maluku 7 Januari 2019. *Jurnal Geosaintek*, *6*(3), 137. https://doi.org/10.12962/j25023659.v

6i3.7030

Toda, S. (2005). Coulomb 3.3 Graphic-rich deformation and stress-change software for earthquake, tectonic, and volcano research and teachin. *USGS Open-File Report*, 63. http://www.coulombstress.org/download

Utama, G., Selama, L., Dan, T., Panjaitan, L. M., Fattah, E. I., Suhendi, C., Wulandari, R., & Perkasa, H. Y. (2020). *Analisis Pergerakan Dan Akumulasi Coulomb Stress*. *7*(1), 35–39.

Wells, Donald L.Coppersmith, K. J. (1994). *No New empirical relationships among magnitude, rupture length, rupture width, rupture area, and surface displacement*. Seismological Society of America, Berkeley, CA, United States. https://doi.org/10.1785/BSSA0840040974